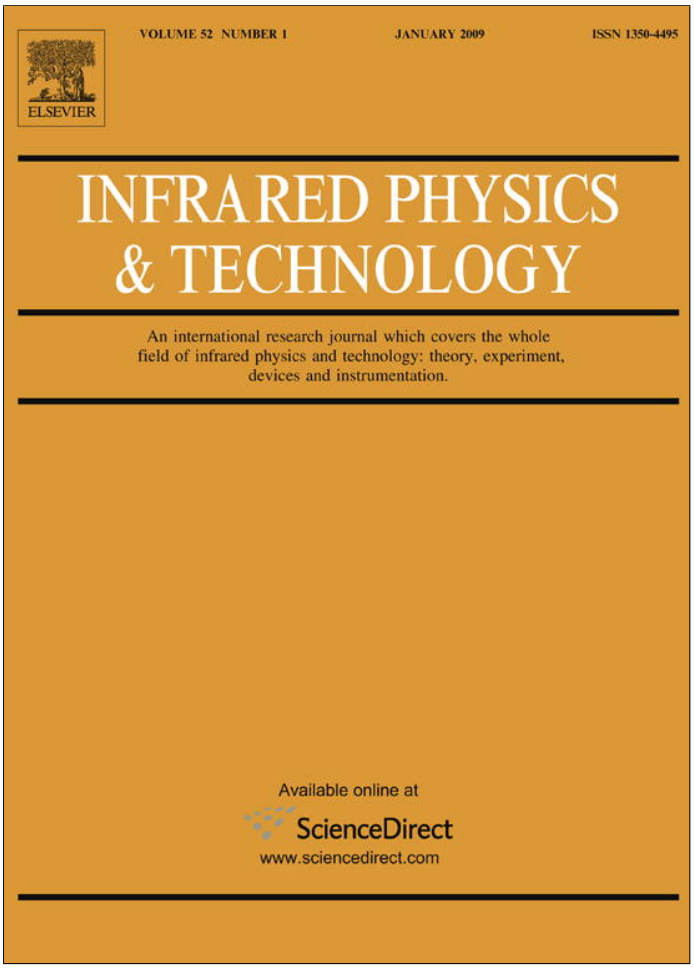

Infrared Physics & Technology 52 (2009) 42–47

Contents lists available at ScienceDirect

Infrared Physics & Technology

journal homepage: www.elsevier.com/locate/infrared

Normalized methodology for medical infrared imaging

J.V.C. Vargas [a,*], M.L. Brioschi [a], F.G. Dias [b], M.B. Parolin [c], F.A. Mulinari-Brenner [d], J.C. Ordonez [e], D. Colman [c]

[a] Programa de Pós-Graduação em Engenharia Mecânica, Departamento de Engenharia Mecânica, Universidade Federal do Paraná, Curitiba, PR, 81531-980, Brazil
[b] Programa de Pós-Graduação em Engenharia, Universidade Federal do Paraná, Curitiba, PR, 81531-980, Brazil
[c] Transplante Hepático, Hospital de Clínicas da Universidade Federal do Paraná, Curitiba, Paraná, 80060-160, Brazil
[d] Departamento de Medicina Interna, Universidade Federal do Paraná, Curitiba, Paraná, 80060-160, Brazil
[e] Center for Advanced Power Systems and Department of Mechanical Engineering, Florida State University, Tallahassee, FL 32310, USA

ARTICLE INFO

Article history:
Received 7 August 2008
Available online 7 December 2008

Keywords:
Dimensionless temperature
Skin thermography
Indeterminate leprosy

ABSTRACT

A normalized procedure for medical infrared imaging is suggested, and illustrated by a leprosy and hepatitis C treatment follow-up, in order to investigate the effect of concurrent treatment which has not been reported before. A 50-year-old man with indeterminate leprosy and a 20-year history of hepatitis C was monitored for 587 days, starting from the day the patient received treatment for leprosy. Standard therapy for hepatitis C started 30 days later. Both visual observations and normalized infrared imaging were conducted periodically to assess the response to leprosy treatment. The primary end points were effectiveness of the method under different boundary conditions over the period, and rapid assessment of the response to leprosy treatment. The patient achieved sustained hepatitis C virological response 6 months after the end of the treatment. The normalized infrared results demonstrate the leprosy treatment success in spite of the concurrent hepatitis C treatment, since day 87, whereas repigmentation was visually assessed only after day 182, and corroborated with a skin biopsy on day 390. The method detected the effectiveness of the leprosy treatment in 87 days, whereas repigmentation started only in 182 days. Hepatitis C and leprosy treatment did not affect each other.

1. Introduction

According to Wallace [1], medical thermography was conceived and first applied to patients by Lawson [2] in Montreal, and reported on two patients with breast cancers, showing increased temperature over the tumor site. Williams et al. [3,4] reported on an infrared survey of 200 cases of breast cancer, also detecting increased temperature on the affected skin regions. These studies might be considered the starting points of medical infrared thermal imaging.

In an attempt to provide objective means to analyze skin surface temperature readings, Collins et al. [5–7] developed the thermographic index to quantify infrared thermal imaging. The method was then utilized in several studies with different disorders [8–12]. All studies showed the effect of medications on the thermographic index, which returned to basal levels with the symptoms remission. In general, the results established the concept of a stable environment as one of a number of essentials to reliable technique.

Other methods for medical infrared imaging quantification have been proposed, such as: (i) a heat distribution index (HDI), which consists of the average skin temperature at the affected region ± the standard deviation of the measurements [13], (ii) a compound thermographic index (CTI) in correlation with low density lymphocytes (LDL) [14,15], (iii) a normalized thermographic index (ΔT_n), which consists of the evaluation of the TI at the affected region minus the TI of a normal selected region [16], and (iv) a $d\tau$ index (difference between temperatures of tissues of a breast tumor and normal tissues) [17]. Inoue et al. [18] evaluated patients with rheumatoid arthritis after 20 min of thermal stabilization in a room at 20 °C showing that the HDI results correlated better with clinical observations than the TI.

An alternative to medical infrared imaging is the so called skin-contact thermography. Recently, a wearable device for skin-contact thermography using silicon sensors was studied by Giansanti [19], who designed a cubic–spline interpolation procedure to improve the spatial resolution of the device. The methodology does not compare to infrared imaging in terms of spatial resolution, but it is required when subjects need to be monitored for 24 h, since the infrared camera cannot be affixed to a body segment or to a breast for 24 h.

The previously proposed methods for medical thermography (TI, HDI, CTI, ΔT_n, $d\tau$, and skin-contact thermography) measure local temperatures that are significantly affected by ambient temperature and patient metabolism. A way to normalize temperature

* Corresponding author. Tel.: +55 41 3361 3307; fax: +55 41 3361 3129.
E-mail address: jvargas@demec.ufpr.br (J.V.C. Vargas).

1350-4495/$ - see front matter © 2008 Elsevier B.V. All rights reserved.
doi:10.1016/j.infrared.2008.11.003

Nomenclature

A_Ω	area of the affected region, m^2
CTI	compound thermographic index, °C
$d\tau$	difference between temperatures of tissues of a breast tumor and normal tissues, °C
HDI	heat distribution index, °C
LDL	low density lymphocytes
MDT	multidrug therapy
ROM	rifampin, ofloxacin, and minocycline single dose indeterminate leprosy treatment
t	time, days
T	skin surface temperature at a point, °C
TI	thermographic index, °C
T_b	central body temperature, °C
T_∞	ambient temperature, °C
x, y	cartesian coordinates, m

Greek symbols

ΔT_n	normalized thermographic index, °C
θ	dimensionless temperature, Eq. (2)
$\bar{\theta}$	average dimensionless temperature, Eq. (4)
Ω	affected region domain, Fig. 1

readings for any specific location would therefore be of much use in medical practice. Normalized infrared imaging could provide means for early and accurate detection of the response to treatment, mainly when other treatments are conducted simultaneously due to co-infections. The literature reports a relatively high prevalence of hepatitis C combined with leprosy in several countries [20,21], but, within the knowledge of the authors, does not document the resulting effect of combined peginterferon alfa-2a and ribavirin on leprosy patients undertaking concurrent multidrug therapy (MDT) and vice versa.

1.1. Objectives of the paper

Two objectives were sought in this work: (i) to suggest a normalized methodology for general thermography interpretation, and (ii) to test the methodology in the treatment follow-up of an indeterminate leprosy and hepatitis C case, for early and accurate detection of leprosy skin lesion evolution.

2. Materials and methods

The methodological flow was divided in three steps:

- The development of the theoretical methodology for normalized infrared imaging.
- The experimental procedure for temperature data acquisition and calculation of uncertainties, and
- The performance evaluation of the suggested normalized infrared imaging methodology with a case study of concurrent hepatitis C and indeterminate leprosy.

2.1. Theory

The energy conservation principle [22] states that, for any time interval, the variation of the energy of a system results from the exchange of matter and energy with the exterior, and the system energy variation is equal and opposite to the external world energy variation. Considering the system as a portion of an individual skin (the region of interest), its energy variation is a result of the exchange of matter and energy with the ambient and the rest of the individual's body. Therefore, since energy is directly related to temperature, a general methodology to interpret the temperature readings obtained from an individual skin should consider the local environmental conditions and the individual metabolism.

An appropriate dimensionless variable was identified to interpret the infrared camera temperature readings. The variable is a well known dimensionless temperature in engineering heat transfer, and combines the locally measured temperature with the central body and ambient temperatures, as follows:

$$\theta = \frac{T - T_\infty}{T_b - T_\infty} \tag{1}$$

The dimensionless temperature defined by Eq. (1) is expected to deliver normalized temperature readings, independently of measuring units, for any particular skin location, whatever body and ambient temperatures are registered. The dimensionless temperature, as defined by Eq. (1), was first introduced in engineering by Pohlhausen [23], who used it to present the normalized temperature profile solution to the thermal boundary layer problem of laminar forced convection on a flat plate.

In addition to the definition of a local measuring quantity, it is necessary to specify a representative quantity for the skin region of interest, namely, the affected region. Fig. 1 shows a portion of the affected skin, in which a polygonal line defines a domain Ω with respect to two Cartesian axes x and y. The polygonal line should be appropriately specified to encompass the entire region of interest. Each region provides a dimensionless temperature field, which depends on x and y, i.e., $\theta(x, y)$. Using the mean value theorem for integrals, the average dimensionless temperature for the entire region of interest is therefore evaluated by:

$$\bar{\theta} = \frac{1}{A_\Omega} \int \int_\Omega \theta(x, y) \mathrm{d}x\mathrm{d}y \tag{2}$$

Eq. (2) defines the quantity to be obtained through the infrared camera temperature readings in the entire selected region of interest, and through the measured central body and ambient temperatures.

2.2. Temperature measurements

The infrared images were obtained using a SAT-S160 Infrared camera, manufactured by SAT (Guangxhou SAT Infrared Technol-

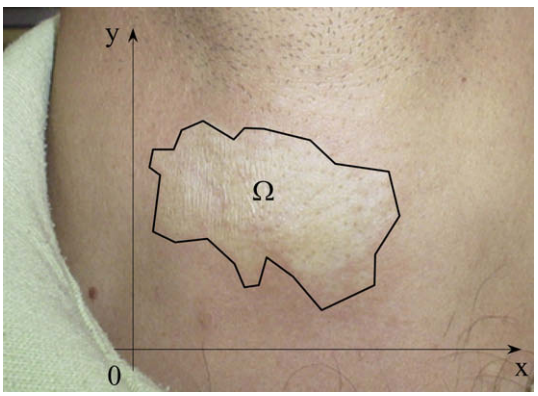

Fig. 1. The skin region of interest, namely, the affected region.

ogy CO., LTD), with a spatial resolution of 2.2 mrad, 160 × 120 pixels, a bias limit of ±2% (temperature accuracy), and a temperature resolution of 0.1 °C. The camera was placed at a horizontal distance of 1 m away from the region of interest on the patient's skin in order to ensure the same view factor and dimensions for the selected region of interest in all thermographs. Although the literature shows discrepancies for the values of human skin emissivity, it was possible to attribute an emissivity of 0.975 to the human skin surface based on relatively recent work [24–26].

The average of the measurements taken with four high precision thermistors of type YSI44004 (YSI Inc., USA), standard type Bead I, with a maximum diameter of 2.4 mm, was utilized to estimate the ambient temperature close to the patient in the testing room, T_∞. A fifth and a sixth thermistor were placed under the two armpits of the individual being tested, and the average of the measurements was used to estimate the patient's central body temperature, $T_b \pm 0.001$ °C. All tests started at least ten minutes after the body temperature thermistors were placed, in order to read the actual body temperature of the subject.

The thermistors were immersed in a constant temperature bath, and sixty-four temperature measurements were made at 20 °C, 30 °C, 40 °C, . . . , 80 °C. The largest standard deviation of these measurements was 0.0006 °C, therefore the bias limit was considered ±0.001 °C for all the thermistors.

The experimental work involved the acquisition of temperature data in real time. This task was performed through the utilization of a computational data acquisition system which consisted of a digital multimeter board, NI PCI-4060, a NI PCI-6703 analog output board, a SCXI-1127 32-channel high voltage multiplexer, and accessories, all manufactured by National Instruments, USA, which allows for the sequential data acquisition from 32 channels at interval times of 0.1 s. All the data were processed by a home made Labview application (National Instruments, USA) to convert the sensors signals in readable temperatures. In this way, the temperature measurements originated from the six thermistors utilized in the experiments were read almost simultaneously, i.e., in less than a second. The program also generated files with the numerical data measured for the patient, and allowed the calculation of the average dimensionless temperature according to Eq. (2), with the region of interest temperature field data obtained with the infrared camera and a bi-dimensional numerical integration procedure (Simpson's rule [27]). With the equipment described in this section, it was possible to measure all required temperatures almost simultaneously and directly calculate the region of interest average dimensionless temperature.

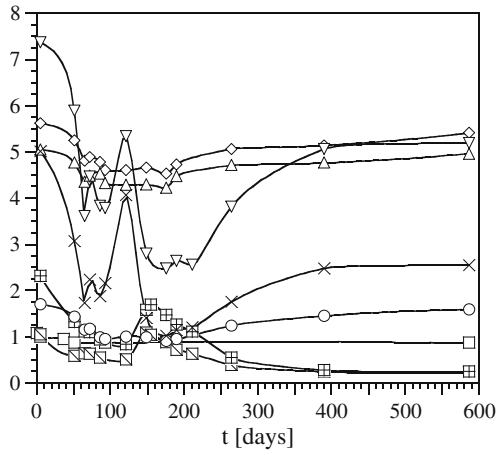

Fig. 2. The patient's response to hepatitis C treatment in time through blood tests: —□— *Fastingglucose* [$\times 10^2$ mg/dl]; —▨— AST [$\times 10^2$ U/l]; —⊞— ALAT [$\times 10^2$ U/l]; —○— Platelet count [$\times 10^{11}$/l]; —◇— Erythrocyte count [$\times 10^{12}$/l]; —△— Hematocrit [$\times 10$]; —▽— Leucocyte count [$\times 10^9$/l]; —×— Absolute neutrophil count [$\times 10^9$/l].

Before the beginning of the experiments, several tests were performed with three different ambient temperatures in an environmentally controlled laboratory, i.e., $T_\infty = 15.5$, 20 and 26 °C. The tests consisted of, for the same individual, to perform the data acquisition of the temperature field on the selected region of interest and body temperature. Then, the value of $\bar{\theta}$ was computed for these three different conditions, resulting in approximately equal values of $\bar{\theta}$ for all cases. Uncertainties were computed based on these three values, taken as the precision limit of the temperature measurements (two times the standard deviation [28]), since the temperature bias limit (±2% of the actually measured temperature with the infrared camera and ±0.001 °C with the thermistors) was considered negligible in presence of the temperature precision limit (at least one order of magnitude smaller). In this way it was demonstrated that the dimensionless group really normalizes the results, making them independent of the ambient and body temperature conditions. For the sake of accuracy, in the present study, the tests were all performed within the ambient temperature range mentioned above, i.e., 15.5 °C $\leqslant T_\infty \leqslant$ 26 °C.

2.3. Case study

A 50 year-old man was referred to an outpatient clinic for treatment of a single lesion with the approximate shape of an ellipse (major axis: 6 cm, minor axis: 4 cm) in the cervical region, as shown in Fig. 1. Microscopy was conducted on a rectified lamellar and epidermis corneal layer, with preserved thickness, measuring 0.3 × 0.3 × 0.3 cm, collected from the affected region. The superficial and deep dermis presented moderate lymphocyte inflammatory infiltrate, with plasmocytes, predominantly perivascular and perineural, sometimes interstitial, with the presence of one acid-fast bacillus. Therefore the patient was diagnosed with indeterminate leprosy. Because of his past history of an untreated chronic hepatitis C and evidence of elevated liver enzymes and positive qualitative HCV–RNA (Cobas Amplicor Hepatitis C Virus Test, version 2.0, Roche Molecular Systems, Branchburg, NJ, USA), a liver biopsy was performed before starting leprosy treatment. The liver specimens showed moderate necroinflammatory activity and advanced fibrosis (METAVIR stage F3). HCV genotyping was determined as 3a (Inno LipA HCV II, Innogenetics, Ghent, Belgium).

The patient was then monitored for 587 days after receiving a single dose of 600 mg of rifampin, 400 mg of ofloxacin, and 100 mg of minocycline, i.e., the so called ROM treatment for indeterminate leprosy. Thirty days later, he started the current standard therapy for hepatitis C [29,30], with 180 μg peginterferon alfa-2a by subcutaneous injection once a week, plus 1000 mg oral ribavirin daily for 24 weeks, achieving sustained virological response 6 months after the end of the treatment, and thereafter (negative quantitative HCV–RNA). Blood tests were utilized to follow the response to the hepatitis C treatment, and both visual and normalized infrared imaging were conducted periodically (0, 15, 28, 46, 59, 73, 87, 144, 182, 204, 257, 367 and 587 days) to assess the response to leprosy treatment. On day 390, a biopsy was conducted on a punch of pink–red skin tissue extracted from the scarred repigmented area, which was soft and elastic, measuring 0.3 × 0.3 × 0.3 cm, showing that the epidermis had no particularities, and that in the mid and deep dermis there was disorganization of thickened collagen groups, with the Ziehl–Neelsen staining method showing no evidence of acid-fast bacilli. The primary end points were the effectiveness of the normalized temperature readings under different boundary conditions over the test period, and the rapid assessment of the response to the leprosy treatment through normalized infrared imaging, while undergoing simultaneous hepatitis C treatment.

3. Results

A recent study [31] still points out the need for an environmentally controlled laboratory and a protocol to ensure consistency for comparing infrared images captured on different occasions (e.g., patient thermal equilibration with the ambient, absence of skin creams). The protocol recommends the thermal equilibration of a patient at a temperature too high for vasoconstriction to occur, but low enough not to mask the effects of inflammation or angiogenesis, which adds a considerable deal of subjectivity to the exam, since no specific temperature levels are established. In time, progress has been made on producing open systems [32,33] for capturing, storing, retrieving, and manipulating sequences of thermal images relating a patient, suggesting three modes of image treatment: (i) single static image at an instant in time to identify hot and cold spots, or asymmetries; (ii) static images on occasions separated by substantial length of time to monitor disease progress or treatment or to detect and estimate the severity of inflammation, and (iii) series of images over a period of minutes to monitor the recovery of skin temperature following a provocation such as thermal, mechanical, or chemical stress. The proposed normalized methodology has the potential to simplify and give more objectivity to infrared imaging protocols in all modes, thus improving the accuracy of image medical interpretation.

The experimental results are shown in Figs. 2–4. The experimentally measured points were interpolated with cubic–splines, for a better visualization of the physical phenomena. The results are organized in a logical sequence, i.e.: (i) regular blood tests to assess the response to hepatitis C treatment; (ii) the physical and infrared images comparison of the monitored leprosy skin lesion,

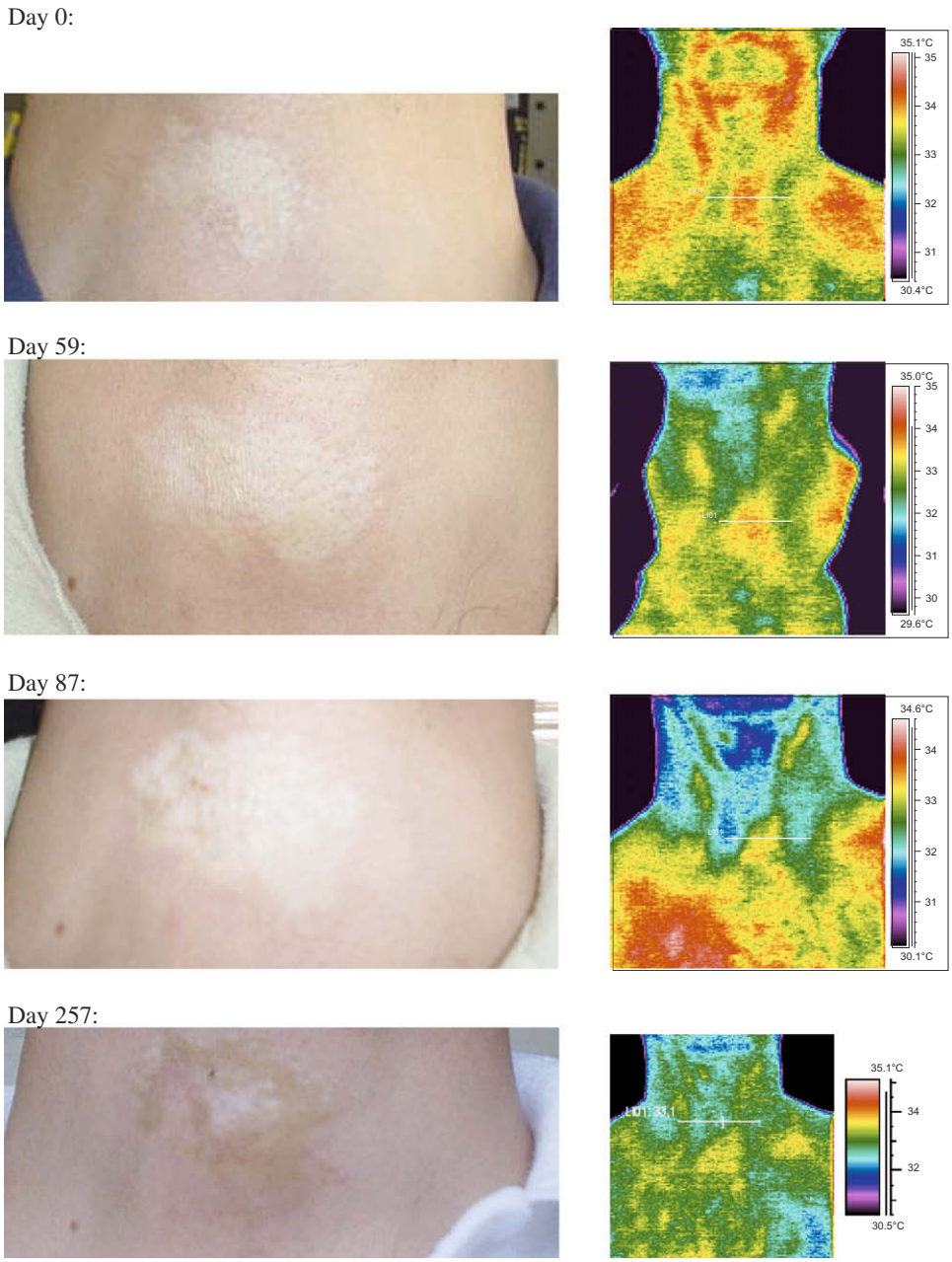

Fig. 3. The correspondence between actual photos and infrared images of the leprosy skin lesion captured on different occasions during treatment follow-up. From top to bottom: day 0, day 59, day 87, and day 257.

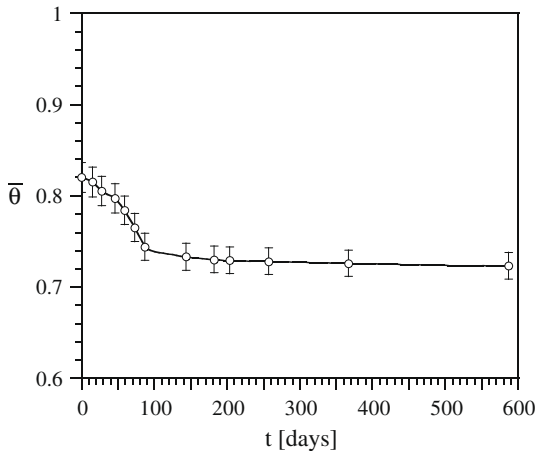

Fig. 4. The patient's average dimensionless temperature response at the skin affected region in time.

and (iii) the skin lesion average dimensionless temperature in time.

Fig. 2 presents a selection of the most representative blood tests monitored during the hepatitis C treatment and the remaining period of observation. Abnormal liver enzyme levels (AST and ALAT) were present in the beginning of the hepatitis C treatment (day 30), which dropped initially, elevated again (day 100), later showing a trend to normal ranges (day 180), i.e., the treatment end point, and indeed stabilizing at normal levels afterwards. Other tests (platelet, erythrocyte, hematocrit, leucocyte, and absolute neutrophil) showed substantial drop during treatment, and stabilizing at normal levels after the end of the treatment. Those results, together with the negative quantitative HCV–RNA demonstrate the hepatitis C treatment success in spite of concurrent leprosy treatment.

Actual photos and infrared images are shown in Fig. 3. The infrared images were obtained with the ambient temperature at 20 °C, and the central body temperature was 36.5 °C in all occasions to ensure consistency for comparing images captured on different days. Four occasions were selected to compare the direct visual and infrared image assessments of the region of interest. On day 0, i.e., when the ROM single dose was taken by the patient, an elevated temperature distribution was observed on the skin lesion, in comparison with the cervical region around it. Since there is immunocytochemical evidence that the initial damage in leprosy is directed at distal, small, unmyelinated nerve fibers, peripheral autonomic dysfunction is expected, resulting in local hyperemia and elevated skin temperature [34]. On day 15, it was seen qualitatively that the temperature distribution on the region of interest dropped to lower values, closer to the surrounding normal skin values, but the lesion remained pale. On day 87, the infrared image shows even lower values than the previous ones, but no lesion repigmentation was observed. On day 257, the temperature distribution was very similar to the previous one, and repigmentation was also in progress. In sum, although a stabilized and fairly uniform temperature distribution was observed from day 87, the skin lesion did not show signs of repigmentation until day 182, which was the day when the skin repigmentation process was detected in the laboratory (not shown in Fig. 3).

Although Fig. 3 documented the decrease in temperature values in the region of interest qualitatively, it would be more instructive for clear medical interpretation if precise quantitative information were available. For that, the region of interest average dimensionless temperature was calculated at 3 different ambient temperature levels, i.e., T_∞ = 15.5,20 and 26 °C, obtaining approximately the same value ($\bar{\theta} \pm 2\%$) on the day the image was taken, showing that the value was indeed normalized in the range of tested ambient temperatures. The procedure was repeated in different occasions (0, 15, 28, 46, 59, 73, 87, 144, 182, 204, 257, 367 and 587 days). The 2% uncertainty was the highest value obtained in all measurements, therefore it was the value used to compute the error bars shown in Fig. 4, where the results are shown graphically. It is observed clearly that after the single dose of the leprosy ROM treatment the average dimensionless temperature started to drop, stabilizing at a lower level after day 87, approximately, and remaining at that plateau until the end of the observation period. The normalized infrared results therefore demonstrate the favorable leprosy treatment outcome in spite of the concurrent hepatitis C treatment, since day 87, whereas repigmentation was visually assessed only after day 182, and corroborated with a skin biopsy on day 390. Since the hepatitis C treatment causes a significant drop in leucocyte and absolute neutrophil count, it was not obvious whether or not the leprosy treatment outcome would be affected by that. Although more concurrent leprosy and hepatitis C cases need to be studied, in the absence of other documented cases, the single case herein studied represents a first assessment that hepatitis C and indeterminate leprosy treatments did not affect each other.

4. Discussion and conclusions

In this study, it was proposed and investigated the utilization of an average dimensionless temperature for infrared imaging analysis. For that, the methodology was theoretically presented and applied to one case study of indeterminate leprosy and hepatitis C. The bulk of the experimental results showed that normalized infrared imaging was able to detect the effectiveness of the leprosy treatment in 87 days, in spite of variable environmental conditions, whereas repigmentation started visually only in 182 days. Combined peginterferon alfa-2a and ribavirin did not affect the patient response to indeterminate leprosy treatment and vice versa. However, for a better assessment of the effects of the leprosy and hepatitis C medications on each other, a larger sample of patients being treated simultaneously for both conditions should be investigated.

The key conclusion is that with a normalized methodology, there is potential for production of analysis criteria for high resolution infrared imaging temperature readings for the diagnosis and follow-up of skin lesions in leprosy treatment, independently of central body and local environmental temperatures, and possibly to all other skin-detectable pathologies, with no need for an environmentally controlled laboratory and complex protocols.

4.1. Future work

Additional research has been planned to show the effectiveness of the normalized thermography methodology for diagnosis and follow-up of all forms of leprosy and possibly other skin-detectable pathologies, and to produce comprehensive dimensionless temperature analysis criteria for them.

Conflicts of interest statement

We declare that we have no conflict of interests.

Acknowledgements

The authors acknowledge with gratitude the support of the Brazilian National Council of Scientific and Technological Development, CNPq.

References

[1] J.D. Wallace, C.M. Cade, Clinical Thermography, CRC, Cleveland, OH, 1975.
[2] R.N. Lawson, Implications of surface temperatures in the diagnosis of breast cancer, Can. Med. Assoc. J. 75 (1956) 309–315.
[3] K.L. Williams, F.L. Williams, R.S. Handley, Infrared radiation thermometry in clinical practice, Lancet 2 (OCT29) (1960) 958–959.
[4] K.L. Williams, R.S. Handley, F.L. Williams, F. Infrared thermometry in the diagnosis of breast disease, Lancet 2 (721) (1961) 1378–1379.
[5] A.J. Collins, E.F.J. Ring, J.A. Cosh, P.A. Bacon, Quantitation of thermography in arthritis using multi-isothermal analysis. I. The thermographic index, Ann. Rheum. Dis. 33 (2) (1974) 113–115.
[6] E.F.J. Ring, A.J. Collins, P.A. Bacon, J.A. Cosh, Quantitation of thermography in arthritis using multi-isothermal analysis. II. Effect of nonsteroidal anti-inflammatory therapy on the thermographic index, Ann. Rheum. Dis. 33 (4) (1974) 353–356.
[7] A.J. Collins, Anti-inflammatory drug assessment by the thermographic index, Acta Thermographica 1 (2) (1976) 73–79.
[8] E.F.J. Ring, Thermographic evaluation of calcitonin therapy in Paget's disease of the tibia, Acta Thermographica 1 (2) (1976) 67–72.
[9] E.F.J. Ring, Computerised thermography for osteo-articular diseases, Acta Thermographica 1 (3) (1976) 166–172.
[10] E.F.J. Ring, P.A. Bacon, Quantitative thermographic assessment of inositol nicotinate therapy in Raynaud's phenomena, J. Int. Med. Res. 5 (4) (1977) 217–222.
[11] F. Beaudet, A.S. Dixon, Posterior subtalar joint synoviography and corticosteroid injection in rheumatoid arthritis, Ann. Rheum. Dis. 40 (2) (1981) 132–135.
[12] S. Zieniuk, B. Stawarz, K. Zieniuk, Infra-red thermography testicular studies of patients with short spermatic cords and quality of sperm morphology, Ginekol. Pol. 69 (6) (1998) 551–554.
[13] R.S. Salisbury, G. Parr, M. De Silva, B.L. Hazleman, D.P. Page-Thomas, Heat distribution over normal and abnormal joints: thermal pattern and quantification, Ann. Rheum. Dis. 42 (5) (1983) 494–499.
[14] G.M. Papadimitriou, P.A. Bacon, N.D. Hall, Circulating activated lymphocytes in rheumatoid arthritis: a marker of synovial inflammation, J. Rheumatol. 9 (2) (1982) 217–223.
[15] G.J. Alexander, P.A. Bacon, F. Cavalcanti, D.R. Blake, N.D. Hall, Low density lymphocytes: their relationship to disease activity and to antirheumatic therapy, Br. J. Rheumatol. 23 (1) (1984) 6–14.
[16] H. Warashina, Y. Hasegawa, H. Tsuchiya, S. Kitamura, K. Yamauchi, Y. Tori, M. Kawasaki, S. Sakano, Clinical, radiographic, and thermographic assessment of osteoarthritis in the knee joints, Ann. Rheum. Dis. 61 (9) (2002) 852–854.
[17] T. Yahara, T. Koga, S. Yoshida, S. Nakagawa, H. Deguchi, K. Shirouzu, Relationship between microvessel density and thermographic hot areas in breast cancer, Surg. Today 33 (4) (2003) 243–248.
[18] K. Inoue, J. Nishioka, T. Kobori, Y. Nakatani, S. Hukuda, The use of thermography in the assessment of the rheumatoid knee – the thermographic index and the heat distribution index, Ryumachi 30 (5) (1990) 356–361.
[19] D. Giansanti, Improving spatial resolution in skin-contact thermography: comparison between a spline based and linear interpolation, Med. Eng. Phys. 30 (2008) 733–738.
[20] H. Rosa, R. Martins, B. Vanderborght, Short report: association between leprosy and hepatitis C infection: a survey in a region of central Brazil, Am. J. Trop. Med. Hyg. 55 (1) (1996) 22–23.
[21] A.C.M. Braga, I.J.M. Reason, E.C.P. Maluf, E.R. Vieira, Leprosy and confinement due to leprosy show high association with hepatitis C in southern Brazil, Acta Tropica 97 (2006) 88–93.
[22] I. Prigogine, D. Kondepudi, Thermodynamique, Éditions Odile Jacob, 1999. ch. 2.
[23] E. Pohlhausen, Der wärmeaustausch zwischen festen körpern und flüssigkeiten mit kleiner reibung und kleiner wärmeleitung, Z. Angew Math. Mech. 1 (1921) 115–121.
[24] J. Steketee, Spectral emissivity of skin and pericardium, Phys. Med. Biol. 18 (5) (1973) 686–694.
[25] T. Togawa, Non-contact skin emissivity: measurement from reflectance using step change in ambient radiation temperature, Clin. Phys. Physiol. Meas 10 (1) (1989) 39–48.
[26] B.F. Jones, A re-appraisal of the use of infrared thermal image analysis in medicine, IEEE Trans. Med. Imaging 17 (6) (1998) 1019–1027.
[27] D. Kincaid, Cheney, Numerical Analysis Mathematics of Scientific Computing, Springer, Berlin, 1991.
[28] Editorial. Journal of heat transfer policy on reporting uncertainties in experimental measurements and results, ASME J. Heat Transfer 115 (1993) 5–6.
[29] D.B. Strader, T. Wright, D.L. Thomas, L.B. Seef, Diagnosis, management and treatment of hepatitis C, Hepatology 39 (4) (2004) 1147–1171.
[30] J.L. Dienstag, J.G. McHutchison, American gastroenterological association technical review on the management of hepatitis C, Gastroenterology 130 (1) (2006) 231–264.
[31] B.F. Jones, P. Plassmann, Digital infrared thermal imaging of human skin, IEEE Eng. Med. Biol. 21 (6) (2002) 41–48.
[32] P. Plassmann, E.F.J. Ring, An open system for the acquisition and evaluation of medical thermological images, Eur. J. Thermol. 7 (4) (1997) 216–220.
[33] E.F.J. Ring, The historical development of temperature measurement in medicine, Infrared Phys. Technol. 49 (2007) 297–301.
[34] A.F. Hoeksma, W.R. Faber, Assessment of skin temperature by palpation in leprosy patients: interobserver reliability and correlation with infrared thermometry, Int. J. Lepr. Other Mycobact. Dis. 68 (1) (2000) 65–67.